The molecular basis for UV vision in birds: spectral characteristics, cDNA sequence and retinal localization of the UV-sensitive visual pigment of the budgerigar (*Melopsittacus undulatus*)

Susan E. WILKIE*†, Peter M. A. M. VISSERS‡, Debipriya DAS†, Willem J. DEGRIP‡, James K. BOWMAKER† and David M. HUNT*[1]

*Department of Molecular Genetics, Institute of Ophthalmology, University College London, 11–43 Bath Street, London EC1V 9EL, U.K., †Department of Visual Science, Institute of Ophthalmology, University College London, 11–43 Bath Street, London EC1V 9EL, U.K., and ‡Department of Biochemistry, Institute of Cellular Signalling, University of Nijmegen, Adelbertusplein 1, 6525 EK Nijmegen, The Netherlands

Microspectrophotometric (msp) studies have shown that the colour-vision system of many bird species is based on four pigments with absorption peaks in the red, green, blue and UV regions of the spectrum. The existence of a fourth pigment (UV) is the major difference between the trichromacy of humans and the tetrachromacy of such birds, and recent studies have shown that it may play a determining role in such diverse aspects of behaviour as mate selection and detection of food. Avian visual pigments are composed of an opsin protein covalently bound via a Schiff-base linkage to the chromophore 11-*cis*-retinal. Here we report the cDNA sequence of a UV opsin isolated from an avian species, *Melopsittacus undulatus* (budgerigar or small parakeet). This sequence has been expressed using the recombinant baculovirus system; the pigment generated from the expressed protein on addition of 11-*cis*-retinal yielded an absorption spectrum typical of a UV photopigment, with λ_{max} 365 ± 3 nm. This is the first UV opsin from an avian species to be sequenced and expressed in a heterologous system. *In situ* hybridization of this sequence to budgerigar retinas selectively labelled a sub-set of UV cones, representing approx. 9 % of the total cone population, that are distributed in a semi-regular pattern across the entire retina.

INTRODUCTION

The range of spectral sensitivities of the visual systems of animals extends from wavelengths shorter than 400 nm in the near UV to above 800 nm in the far red, with some species utilizing almost this entire spectral range, but others being more restricted within these broad limits [1]. Vision across this spectral range is achieved by a number of different visual pigments that share a common structure and evolutionary origin. All vertebrate visual pigments are composed of an opsin protein covalently bound via a Schiff-base linkage to a chromophore that, in most terrestrial vertebrates and exclusively in birds, is 11-*cis*-retinal. The opsin proteins of vertebrate pigments can be assigned to a maximum of four classes, based on peak sensitivity (λ_{max}), sequence homology and phylogenetic identity [2]. This classification places the so-called red and green cone pigments of humans into a single longwave class, along with the red-sensitive cone pigments of fish, birds and reptiles. The pigments of rod photoreceptors are grouped into a second class along with the rod-like green-sensitive cone pigments of fish, birds and reptiles. The blue-sensitive cone pigments of fish and birds form a third class, and a fourth class comprises the shortwave-sensitive cone pigments of mammals (so-called blue-sensitive), together with the violet cone pigments of the chicken [3] and *Xenopus laevis* [4], the SW1 pigment of the American chameleon [5] and the UV-sensitive cone pigment of the goldfish [6]. In general, birds exhibit a very highly developed colour vision system involving cone pigments from all four classes. Recent studies have shown that vision in the UV may play a determining role in such diverse aspects of behaviour as mate selection [7] and detection of food [8].

In the budgerigar, four cone pigments classified as red, green, blue and UV have been identified by microspectrophotometry (msp) [9]. The budgerigar retina contains a complex assortment of photoreceptor cells, including rods, double cones and at least four classes of single cone each containing only one pigment type. The different cone types are also characterized by the presence of coloured oil droplets, located in the distal ellipsoid region of the inner segment, which act as selective cut-off (long pass) filters interposed between the incident light and the pigment. The UV pigment as measured by msp has a λ_{max} of 371 ± 5 nm and occurs in a sub-population of cells with UV-transparent (T type) oil droplets. UV pigments have also been identified in Pekin robin (*Leiothrix lutea*) [10] and zebra finch (*Taeniopygia guttata*) [9] but are not found universally in all avian species. Thus the shortest-wave pigment to have been identified in chicken (chicken violet) has a λ_{max} of 418 nm [10], whereas those in the Humboldt penguin (*Spheniscus humboldti*) [11] and Manx shearwater (*Puffinus puffinus*) (J. K. Bowmaker, unpublished work) lie in between. UV pigments have also been identified by msp in fish [12] and some reptiles [13], and there is electrophysiological evidence for UV sensitivity in rodents [14] and some amphibians [15].

Our study of the UV pigment of the budgerigar was aimed at answering a number of fundamental questions. (1) Given the large differences in λ_{max} between the chicken violet and budgerigar UV pigments (approx. 50 nm), how closely related are their respective opsin genes and what are their evolutionary origins? (2) If the two genes are related genetically, how do the two opsins succeed in tuning their respective pigments to such different wavelengths? (3) What is the distribution and frequency of UV-sensitive cones in the budgerigar retina?

Abbreviations used: msp, microspectrophotometry; RACE, rapid amplification of cDNA ends.

[1]To whom correspondence should be addressed.

The nucleotide sequence reported in this paper has been submitted to the EMBL Nucleotide Sequence Database under the accession number Y11787.

MATERIALS AND METHODS

cDNA cloning and sequencing

The retinas from wild-type budgerigars were dissected out and chilled quickly on ice before immediate use or storage at −80 °C. mRNA was extracted from this retinal tissue using a Pharmacia QuickPrep Micro mRNA Purification Kit. Single-stranded cDNA was synthesized using an oligo dT primer according to the Gibco–BRL 3′ rapid amplification of cDNA ends (RACE) system. This cDNA was used as template in a PCR using a pair of degenerate oligonucleotide primers designed from the sequence of the chicken violet opsin [3] and *Taq* DNA polymerase to amplify a 952 bp opsin cDNA sequence. The sequence (IUB codes) of the forward and reverse primers used were, respectively, 5′-TGGGCCTTCTACCTMCAG-3′ (v88+) and 5′-TGGCTG-GWGGASACRGAGGA-3′ (cons1040−). This partial opsin sequence was inserted into pTAg (Invitrogen) and fully sequenced. The sequence was identified as the presumptive short-wave opsin sequence on the basis of nucleotide and amino acid similarity with chicken violet opsin. Two gene-specific primers were designed from this partial opsin sequence (BUV273−, 5′-GACGAAGACGGTGAAGATGCA-3′; and BUV833+, 5′-CGACCTGCGCCTCGTCA-CCA-3′) and were used in 5′- and 3′-RACE amplifications (Gibco–BRL) both at 64 °C to obtain further fragments of 257 and 342 bp respectively. These again were inserted into the cloning vector pTAg (Invitrogen) and sequenced and were shown to contain the 5′ and 3′ ends of the coding sequence and short regions of untranslated sequence. To eliminate the possibility of errors being introduced during the PCR, cloned fragments from three independent PCRs were sequenced throughout.

Sequence analysis

Geneworks™ was used for DNA sequence alignments and translations. Protein and nucleotide sequence alignments were performed with Clustal V [16] using default fixed-gap and floating penalties and unweighted for transitions. A phylogenetic tree was generated by the neighbour-joining method [17] from the frequency of nucleotide substitutions between the cDNA sequences of vertebrate opsins, using the *Drosophila Rh*3 opsin (EMBL Nucleotide Sequence Database accession number P04950) as an outgroup. Support for internal branching was assessed by bootstrapping with 500 replicates. Geneworks™ was used to generate a Kyte–Doolittle hydrophobicity plot using a window of 11 residues.

Expression of recombinant budgerigar UV opsin using baculovirus

The complete coding sequence of the UV opsin gene plus a 3′ six-histidine tag was amplified from budgerigar retinal cDNA by PCR using *Pfu* DNA polymerase and the following primer pair: BUV5+, 5′-GCGCGGATCCAATAATGTCGGGTGAGGA-GGAGTTTTAC-3′; and BUV3−, 5′-GCCGGAATTCTCA-GTGATGGTGATGGTGATGGCTGGGGCTGACCTGG-CTGGA-3′. This amplified fragment was inserted into the *Bam*HI and *Eco*RI sites of the baculovirus transfer vector pVL1393 (Pharmingen) and fully sequenced. No PCR incorporation errors were found. The recombinant transfer vector was then co-transfected with Bac-N-Blue viral DNA (Invitrogen) into Sf9 insect cells. Recombinant baculovirus was isolated and purified by three subsequent plaque assays.

Insect cells were grown in 250 ml spinner flasks (Belco) and infected with the recombinant baculovirus. The His-tagged budgerigar opsin was recovered 3 or 4 days post-infection in a total cell membrane preparation. All subsequent operations were carried out in dim red light (Schott RG610 cut-off filter). The visual pigment was generated *in situ* by the addition of 11-*cis*-retinal [18]. It was then extracted into buffer [20 mM bis-Tris propane, 0.5 M NaCl, 20 % (v/v) glycerol, 5 mM β-mercaptoethanol and 2 μg/ml leupeptin, pH 7.0] containing 1 % (w/v) Chaps (Sigma). Partial purification was achieved by immobilized metal-affinity chromatography through a Ni^{2+}-nitrilo-tri-acetate (Qiagen) column. To increase the affinity of the His-tagged pigment for the matrix, the extract was diluted with 1 vol. of 1 % (w/v) dodecylmaltoside (Anatrace) in the same buffer and applied to the column. The column was washed with the same buffer containing 0.5 % (w/v) Chaps/0.5 % (w/v) dodecylmaltoside until no free 11-*cis*-retinal was detected in the eluate. To elute the pigment off the column, 50 mM histidine was added to the buffer, as well as 0.4 mg/ml bovine retina lipids, isolated as described previously [19], to stabilize the eluted pigment. Fractions containing photopigment were identified from their UV–Vis absorption spectra and by Western immunoblotting using an anti-His-tag antibody (CERN9416 [18]).

Spectra were recorded over the 250–650 nm region first in the dark and then after exposure to white light for 3 min. Similar spectra were also recorded after addition of hydroxylamine in the dark to a concentration of 10 mM. For the acid-denaturation experiment, the dark spectrum was first recorded in the presence of 10 mM hydroxylamine and again after the addition of 1 M hydrochloric acid to a pH of 1.9. Subtraction of the two spectra [(after acidification)−(before acidification)] yielded a dark acid-denaturation difference spectrum. This was, however, distorted due to pH effects on protein absorbance and micellar light scattering. To compensate for this, a corresponding light acid-denaturation difference spectrum was obtained by illuminating the sample before acid denaturation. Subtraction of these two difference spectra (dark−light) yielded an undistorted difference spectrum showing the spectral change occurring upon acidification in the dark.

Analysis of retinal in the purified pigment was performed using the stereospecific oxime extraction procedure followed by HPLC separation [20].

In situ hybridization studies

Fragments of 350 bp from budgerigar UV and rod opsin [21] cDNA sequences were amplified from single-stranded budgerigar retinal cDNA and inserted in the sense orientation into the *Eco*RI and *Kpn*I sites of pBS KS+ (Stratagene). The plasmids were linearized using *Eco*RI and *Kpn*I for the preparation of anti-sense and sense probes respectively. Anti-sense and sense cRNA riboprobes were synthesized by run-off transcription from the T3 and T7 promoters, respectively, with digoxygenin-UTP using a DIG RNA labelling kit (Boehringer Mannheim).

Budgerigar retinas were fixed in the eye cups with paraformaldehyde and were then either flat-mounted whole on to microscope slides or prepared for cryosections [22]. The retinas used for whole mounts were from albino (lutino) budgerigars that lack melanin pigment and thus have a non-pigmented retinal epithelium. The whole mounts but not the cryosections were pretreated for 30 min with proteinase K (10 μg/ml) before hybridization. Hybridizations were conducted at 68 °C in hybridization buffer containing 50 % formamide, 5 × SSC, 0.1 % (w/v) *N*-lauryl sarcosine, 0.2 % SDS (w/v) and 1 ng/ml probe. After washing to high stringency, hybrids were revealed using a DIG Nucleic Acid detection kit (Boehringer Mannheim) by incubation with anti-digoxygenin Fab fragments conjugated to alkaline phosphatase and detection with 5-bromo-4-chloro-3-indolyl

phosphate and Nitro Blue Tetrazolium salt. Slides were coverslipped under 100 % glycerol.

Analysis of oil droplets

Retinas were removed from lutino birds, cut into four quadrants and immediately flat mounted on to slides, photoreceptor layer up, under PBS/0.1 % (w/v) Tween. The preparations were viewed with a light microscope under visible and UV (340–380 nm with a 430 nm cut-off) light. The oil droplets in different cell types are distributed in distinct layers, some deeper than others [23] and therefore come into focus at different depths of the field. To overcome this problem, slide photographs were taken of the same field of view at two different focal planes. These were then superimposed in order to build up a complete two-dimensional image of the complement of cones within that particular area of the retina.

RESULTS AND DISCUSSION

Isolation and sequence analysis of the UV opsin cDNA from budgerigar

In order to isolate the UV opsin gene from budgerigar, a PCR-based DNA-amplification approach was chosen using degenerate primers designed from the sequence of the chicken violet opsin [4]. A partial opsin cDNA sequence was amplified by reverse transcriptase PCR (RT-PCR) using retinal poly(A^+) RNA from budgerigar as template. This was identified as a presumptive shortwave opsin sequence on the basis of nucleotide and amino acid similarity with chicken violet opsin. Using sequence data obtained from this first cDNA fragment to design gene-specific primers, the complete cDNA sequence was obtained using the 5′- and 3′-RACE techniques.

The cDNA encodes a 347-residue protein, the predicted secondary structure of which is shown in Figure 1. This structure has the usual opsin characteristics [24], including seven hydrophobic transmembrane helices, a conserved retinal-binding site in helix VII (Lys-291), a glutamate residue in helix III (Glu-108) at the same position as the glutamate counterion in bovine rhodopsin [25], two conserved cysteines (Cys-105 and Cys-182), which are important for the formation of a disulphide bridge, a conserved ERY motif at the junction of helix III and the second cytoplasmic loop required for G-protein binding, putative glycosylation (Asn-12-Gly-13-Ser-14) and palmitoylation (Cys-317) sites, and a serine-rich region near the C-terminus serving as a potential phosphorylation site.

The primary structure of the predicted protein has 84.1 % identity with chicken violet and much lower identity (around 50 %) with other chicken opsins. Phylogenetic analysis of this budgerigar opsin cDNA with other vertebrate opsin cDNA sequences clearly places it in the same clade as the chicken violet, *Xenopus* violet, goldfish UV and mammalian 'blue' opsins, and quite distinct from the other classes of opsins found in vertebrates (Figure 2). The initial branching of the tree within the clade

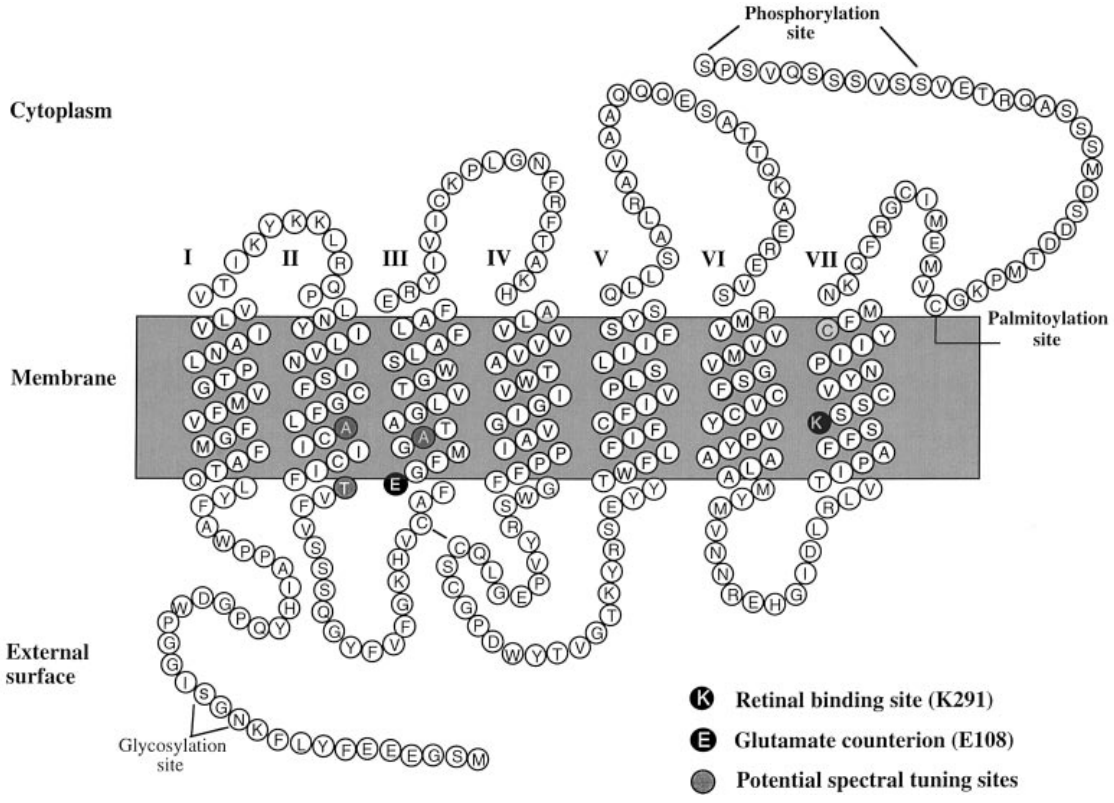

Figure 1 Two-dimensional model of the budgerigar UV-sensitive opsin

Each α-helical region is shown as 26 residues in length, although only the central 18 are thought to be embedded in the membrane. The sites of the retinal Schiff-base linkage (Lys-291) and the potential Schiff-base counterion (Glu-108) are highlighted in black. The disulphide linkage between Cys-105 and Cys-182 is shown, and the positions of the potential glycosylation, palmitoylation and phosphorylation sites are indicated. Potential UV spectral tuning sites are shaded.

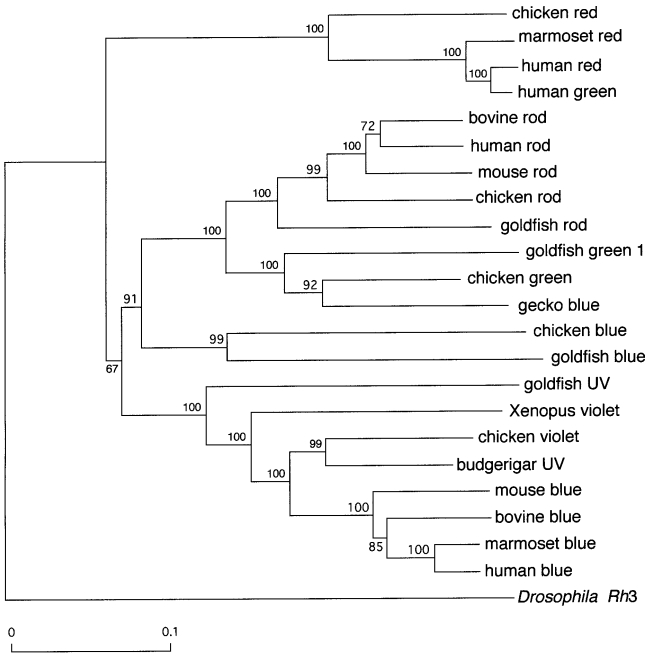

Figure 2 Phylogenetic tree of vertebrate opsins

The tree was generated by the neighbour-joining method [17] from the frequency of substitutions between the nucleotide sequences of the budgerigar UV opsin, the rod (EMBL Nucleotide Sequence Database accession number D00702), red (M62903), green (M92038), blue (M92037) and violet (M92039) chicken opsins, the rod (L11863), red (L11867), green 1 (L11865), blue (L11864) and UV (D85863) goldfish opsins, the rod (U49742), red (M13301), green (K03493) and blue (U53874) human opsins, the red (Z22218) and blue (L76201) opsins from marmoset, the *Xenopus* violet opsin (U23463), the mouse blue opsin (U49720) and the bovine (U92557) blue opsin, using the *Drosophila* Rh3 opsin (P04950) as an outgroup. The bootstrap confidence values based on 500 replicates are shown for each branch. The scale bar is calibrated in substitutions per site.

separates first the goldfish UV and then the *Xenopus* violet from the terrestrial vertebrate sequences. In addition, the UV-sensitive mouse 'blue' groups with the longer-wave mammalian 'blue' opsins. This leaves open the question of whether the ancestral gene giving rise to the four lineages (birds, mammals, amphibians and fish) was violet or UV sensitive. It does, however, suggest that evolution of UV (or violet) sensitivity may have occurred separately in each lineage. Since the mechanism of evolution may differ, the amino acids responsible for spectral tuning of these shorter-wave pigments may also differ between lineages. Thus any search for residues implicated in spectral tuning of the avian UV and violet pigments should focus on avian sequences only.

Heterologous expression of the budgerigar cDNA sequence

Confirmation that the budgerigar sequence encodes a UV-sensitive opsin was obtained by heterologous expression in the recombinant baculovirus system. The cDNA coding sequence used to generate recombinant virus was extended with six histidine codons (a His-tag) immediately upstream of the stop codon. Such a His-tag was shown not to affect the spectral properties of the human red and green cone pigments [18]. Infection of Sf9 insect cells with the purified recombinant virus resulted in the production of a recombinant protein of size in the range 36–39 kDa as demonstrated by Western-immunoblot analysis using an anti-His-tag antibody (Figure 3a). This is the expected apparent size of a visual opsin carrying one Asn-linked saccharide moiety [18]. After generation of the pigment by adding the chromophore (11-*cis*-retinal) to the recombinant protein, the His-tag was used to purify the pigment using affinity chromatography on a nickel column [26]. The pigment eluted off the column was incorporated into mixed micelles using a buffer that contained detergents (Chaps and dodecylmaltoside) and retina lipids. The fractions containing His-tagged protein were again identified by Western-immunoblot analysis using the anti-His-tag antibody (Figure 3a) and were subjected to spectral analysis (Figures 3b and 3c). Only fractions containing the anti-His-tag antibody-reactive band showed a typical near-UV absorbance peak (see below). Using this method, purification of the pigment was achieved in a single stage to a sufficient extent to allow spectral analysis.

The dark spectrum of the fractions containing the His-tagged protein shows an absorption profile that could represent a UV photopigment. The data for the dark spectrum of the purified pigment were fitted to two rhodopsin template curves [27,28] and yielded a best estimate for λ_{max} of 365 ± 3 nm (Figure 3b). A corresponding experiment in which all-*trans*-retinal was substituted for 11-*cis* did not produce any absorption at 365 nm upon elution of bound protein.

The most characteristic feature of a visual pigment is its photosensitivity. Illumination leads to the isomerization of the chromophore from the 11-*cis* to the all-*trans* form, with the subsequent generation of the active state (Meta II) within milliseconds. In mixed micelles Meta II decays rapidly to release free all-*trans*-retinal [29]. HPLC analysis demonstrated the presence of 11-*cis*-retinal in the unbleached pigment, which was almost completely converted to the all-*trans* isomer following illumination (results not shown). It is more difficult, however, to demonstrate by spectrophotometry the photosensitivity of a UV pigment. This is because both Meta II and any all-*trans*-retinal released from the pigment on bleaching will have a λ_{max} in the range 370–380 nm, very close to that of the pigment itself, and the molar absorbances would also be expected to be very similar [29]. Nonetheless a small shift of the expected magnitude was observed on bleaching, albeit in a noisy spectrum, indicative of a photoproduct absorbing at a somewhat higher wavelength than the pigment itself (Figure 3c). Addition of 10 mM hydroxylamine to convert Meta II and free retinal into retinal oxime (λ_{max} 365 nm) predictably failed to show a clear shift in the peak upon illumination.

To overcome these difficulties in explicitly demonstrating that the 365 nm absorption in the dark spectrum represents a photopigment, an alternative approach was adopted. Acid denaturation of the opsin in the pigment by acidification in the dark to pH 1.9 will abolish the spectral tuning of the chromophore, while maintaining the integrity of a protonated Schiff-base linkage, and the λ_{max} would be expected to shift to approx. 440 nm [29]. Figure 3(d) (curve 1) shows the effect of such an acidification in the dark to pH 1.9 in the presence of 10 mM hydroxylamine. At this concentration, hydroxylamine will react slowly with the pigment in the dark and very slowly with the protonated Schiff base generated after acidification. In the resulting difference spectrum [(before acidification) subtracted from (after acidification)], in addition to baseline distortion in the UV region due to acidification, a peak is apparent near 440 nm, indicative of the presence of a simple protonated Schiff base. If the pigment is illuminated before acidification, only baseline distortions due to acidification are seen (Figure 3d, curve 2), since the retinal released from the pigment on illumination will be rapidly converted to retinal oxime, which is not protonated at this pH. Subtraction of curve 2 from curve 1 yields the spectral change occurring upon acidification in the dark state only, undistorted by baseline changes (Figure 3d, bottom panel). This clearly

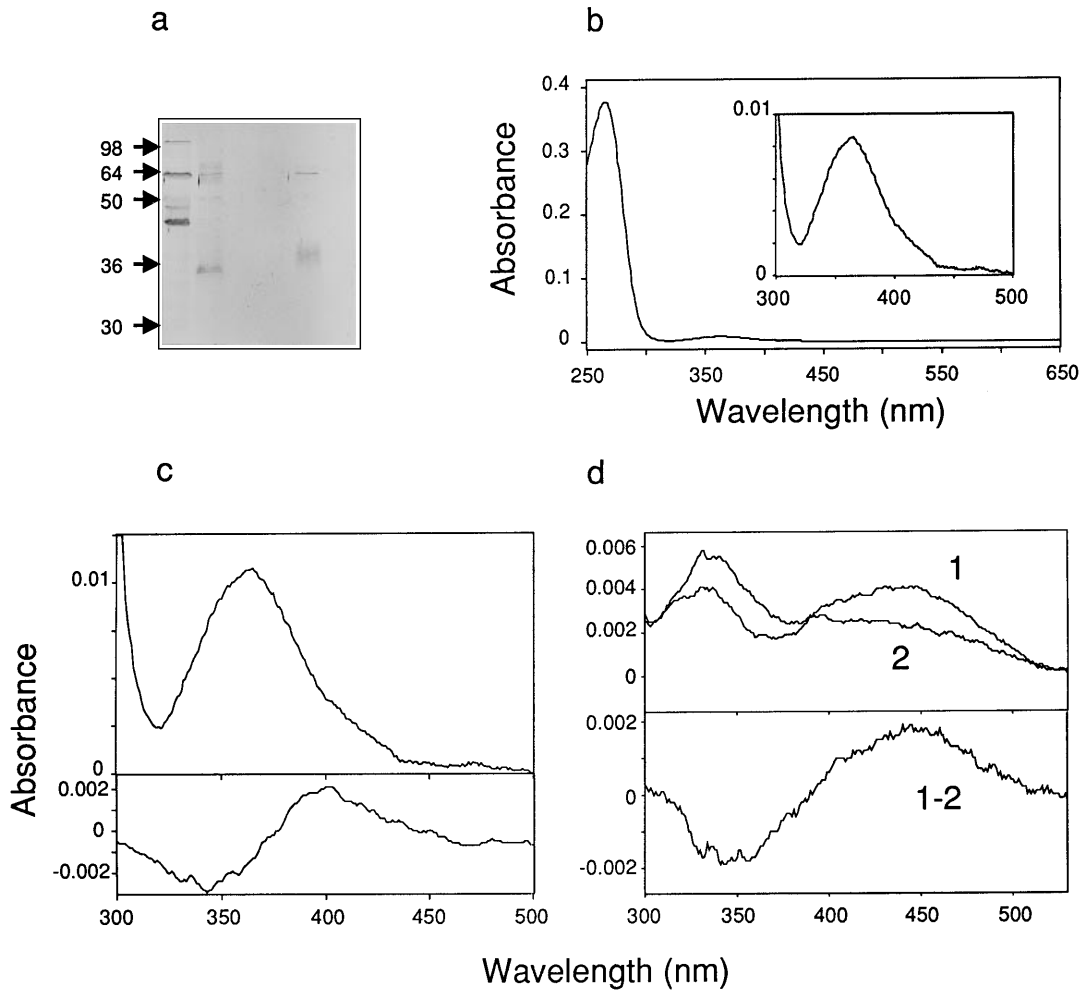

Figure 3 Analysis of recombinant budgerigar UV pigment expressed using the heterologous baculovirus system

(**a**) Western-immunoblot analysis using an anti-His-tag antibody: lane 1, non-infected Sf9 insect cells; lane 2, crude membrane extract from Sf9 cells expressing His-tagged budgerigar opsin; lanes 3 and 4, wash fractions from the Ni^{2+}-nitrilo-tri-acetate acid column; lane 5, peak fraction containing partially purified UV pigment; and lane 6, fraction collected after elution of the pigment. Arrows indicate the positions of protein size markers (in kDa). The mobility of the partially purified His-tagged protein in lane 5 is reproducible and corresponds to that observed with other His-tagged cone pigments generated in our laboratory [18]. The mobility of the protein in the crude extract in lane 2 is more variable, due to the high protein loading in this lane of the gel and does not always correspond exactly to that of the more purified protein. The sharp band around 60 kDa in lanes 2 and 5 represents an endogeneous protein that cross-reacts with the antiserum. Infection with non-recombinant virus produces an immunoblot very similar to lane 2, except that the pigment band near 36 kDa is absent (not shown). (**b**, **c**) UV–Vis absorption spectra of fractions containing purified His-tagged UV pigment. (**b**) Dark spectrum of the purified pigment with (inset) a magnification of the pigment absorbance peak (λ_{max} 365 $\pm$ 3 nm). (**c**) Magnification of the pigment absorbance peak (upper curve) with, in the lower curve, the difference spectrum obtained by subtracting the dark spectrum from that obtained after illumination with white light. This demonstrates that photobleaching is accompanied by a small red shift in absorbance. (**d**) Difference spectrum of the pigment after acid denaturation to pH 1.9 in the presence of 10 mM hydroxylamine (curve 1) and the corresponding difference spectrum obtained when the pigment is first illuminated with white light before acid denaturation in the presence of 10 mM hydroxylamine (curve 2). Lower curve (1–2) represents the difference spectrum of these two acid-denaturation difference spectra (curve 1 — curve 2). A positive peak appears at approx. 440 nm indicative of the formation of a simple protonated Schiff base, and a negative peak at 365 nm corresponds to the loss of the UV pigment. The noise results from the sequential spectral subtraction.

shows the transition from a peak in the UV (negative peak) to one absorbing around 440 nm (positive peak). Such a behaviour would only be exhibited by a retinal-based photosensitive pigment, and we conclude, therefore, that the spectrum produced in Figure 3(b) represents the absorption spectrum of a partially purified UV photopigment with a λ_{max} of 365 $\pm$ 3 nm. This result is very close to the value of λ_{max} obtained for the native pigment by msp (371 $\pm$ 5 nm) [9], the small discrepancy between the two figures falling within the limits of experimental error. Because of the low thermal stability of the photopigment, we have only been able to achieve a partial purification so far, as evidenced by the high A_{260}/A_{365} ratio in the spectrum. However, the result serves to confirm the identity of the opsin sequence used to generate the recombinant photopigment as the budgerigar UV opsin.

Spectral tuning of the budgerigar opsin to the UV

We have addressed the question of which amino acid residues in the budgerigar opsin might be responsible for tuning the λ_{max} of the pigment to 365–371 nm by comparing the sequence to that of the chicken violet pigment (λ_{max} 418 nm). Previous work on vertebrate visual pigments has shown that most of the amino acid changes that affect λ_{max} are located in the transmembrane helices and are non-conservative, i.e. they involve either a change

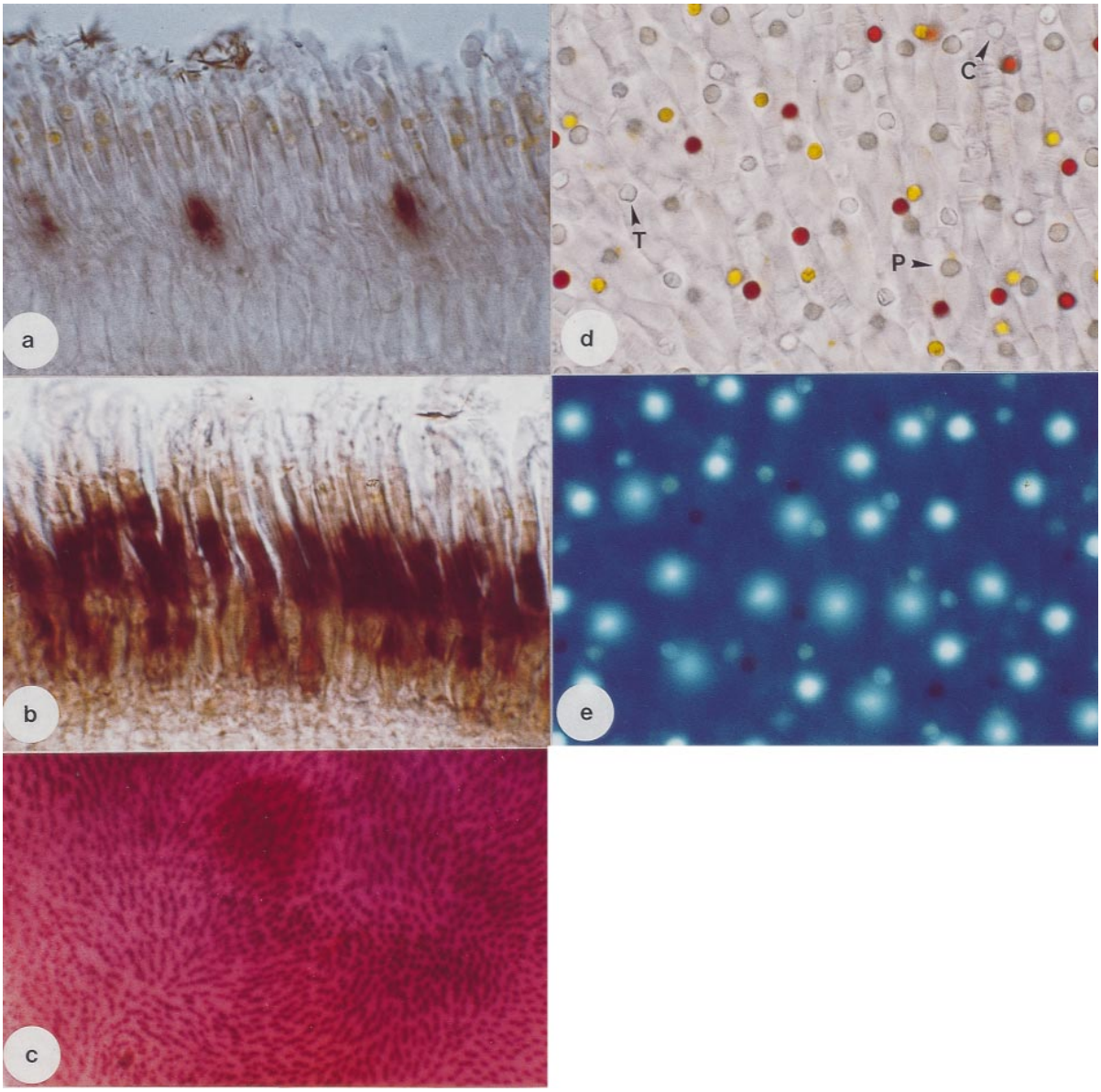

Figure 4 Localization of UV cones in the budgerigar retina by *in situ* hybridization and oil-droplet fluorescence

In situ hybridization to cryosections (**a**, **b**) and whole mount (**c**) with UV (**a**, **c**) and rod (**b**) riboprobes. The probes were of anti-sense RNA and hybridized to complementary mRNA in the cells. Control (sense) probes showed no hybridization signal (not shown). Oil droplets were viewed under (**d**) visible and (**e**) UV light. Under visible light the P-, C- and T-type droplets all appear white or slightly greenish, depending on the focussing level. However, under UV light, the T-type droplets may be distinguished from the others, since they give no fluorescence.

of charge or the gain/loss of a hydroxyl group [30,31]. Using the three-dimensional model of G-protein-linked receptors proposed by Baldwin [32] to identify the seven transmembrane helices, five sites were found where non-conservative substitutions have occurred (A81S, T88V, A113T, T114H and S293A in budgerigar UV/chicken violet respectively). Site 114 can be eliminated, since it is not situated on the inner face of the helix in a position to interact directly with the chromophore. Three of the remaining sites (81, 88 and 113) are in the vicinity of the glutamate residue (Glu-108), which occurs at the same position as the glutamate counterion to the protonated Schiff base in longer-wave photopigments (Figure 1) [25]. From the position of the λ_{max} and the narrow half-band width of the α-band, it has been suggested that the Schiff base is unprotonated in UV pigments [33]. If this is the case, then the effect of Glu-108 in the budgerigar pigment would have to be neutralized by electrostatic interactions with nearby residues. Alternatively, a very weakly protonated Schiff base could be present, stabilized by a hydrogen-bonded network, with proper modulation of the dielectric constant and dipolar interaction with the chromophore to blue-shift the absorbance into the UV region [34].

In situ localization of the UV cones in the budgerigar retina

The localization of the UV cones in the budgerigar retina was investigated by *in situ* hybridization. Digoxygenin-labelled riboprobes, prepared from 350-base fragments of budgerigar UV and rod (control) opsin cDNAs, were hybridized to cryosections and

Table 1 Distribution of cone cells in the budgerigar retina

Cell type	Oil-droplet type	Cells counted	Percentage of total cones
Double cones	P	287	39.9
Single cones-red	R	145	20.1
Single cones-green	Y	153	21.3
Single cones-blue	C	70	9.7
Single cones-UV	T	65	9.0

whole retinas from budgerigar. The UV probe hybridized to a subset of small cone cells identified as presumptive UV cones (Figure 4a). The signal was confined to the inner segment around the nucleus and the region of the outer limiting membrane. In comparison, the cells to which the rod probe hybridized were more numerous and larger in size, and the signal occupied almost the entire length of the inner segment (Figure 4b). Since both probes were of comparable sensitivity when tested on a DNA dot blot (results not shown), the difference in signal between these presumptive UV and rod cells indicates that the amount of opsin message in the smaller UV cones is much less than in the rods.

The retinal whole mounts that had been subjected to *in situ* hybridization revealed a uniform spread of UV cones across the retina (Figure 4c). There appears to be some degree of regularity in the arrangement of the UV cones in budgerigar, somewhat reminiscent of the semi-regular array of blue cones found in the human retina [35], although with fewer gaps, and distinct from the simple rectangular geometry of the cone mosaic in the goldfish retina [36].

In order to assess the relative frequency of UV cones in the budgerigar retina, an analysis was made of the oil droplets present in the cone cells. Under visible light (Figure 4d) four types of single cone (red, green, blue and UV) were visible, containing red-, yellow-, clear- (C) and transparent- (T) type droplets respectively, as well as double cones containing pale- (P) type droplets [9]. However, because of chromatic aberration, the P-, C- and T-type droplets all appear rather similar (white or slightly greenish) and are hard to distinguish. This difficulty was overcome by viewing under UV illumination (Figure 4e) according to Ohtsuka's method [37]. Under these conditions, the P droplets gave an intense white fluorescence, the C droplets gave a much fainter white fluorescence, and the T droplets gave no fluorescence at all. Hence the identity of all the cone types could be inferred from the optical properties of the oil droplets.

The number of cone cells of each type was estimated by counting the numbers of each oil-droplet type within several sectors distributed across the entire retina. As shown in Table 1, the budgerigar retina is dominated by the longer-wave red and green cones. However, the UV cones make up a substantial contribution to the total cone-cell population at about 9%, approximately equal to that of the blue cones. This observation of a 1:1 UV-to-blue cone ratio was further confirmed by comparing the results of *in situ* hybridizations of whole mounts with the UV riboprobe and with a budgerigar blue-cone opsin riboprobe (results not shown). The presence of substantial UV sensitivity across the whole visual field is consistent with the notion that the budgerigar uses its UV vision for a range of functions and contrasts with the sparse distribution of UV-sensitive cones in the mouse, which shows a clear localization in the ventral retina [38].

Received 29 August 1997/29 October 1997; accepted 11 November 1997

This work was supported by grants from the BBSRC to J.K.B. and D.M.H. and from the HFSP (RG 68/95) to W.J.D. We thank Jenny VanOostrum for performing the HPLC analyses and Robert Alexander for assistance with the cryosections.

REFERENCES

1 Bowmaker, J. K. (1991) in Vision and Visual Dysfunction, 2, Evolution of the Eye and Visual System, (Gregory, R. L. and Cronly-Dillon, J. R., eds.), pp. 63–81, Macmillan, London
2 Bowmaker, J. K. and Hunt, D. M. (1998) in Adaptive Mechanisms in the Ecology of Vision (Archer, S. N., Djamgoz, M. B. A., Loew, E., Partridge, J. C. and Vallerga, S., eds.), Chapman and Hall, London, in the press
3 Okano, T., Kojima, D., Fukada, Y., Shichida, Y. and Yoshizawa, T. (1992) Proc. Natl. Acad. Sci. U.S.A. **89**, 5932–5936
4 Starace, D. M. and Knox, B. E. (1997) J. Biol. Chem. **272**, 1095–1100
5 Kawamura, S. and Yokoyama, S. (1996) Vision Res. **36**, 2797–2804
6 Hisatomi, O., Satoh, T., Barthel, L. K., Stenkamp, D. L., Raymond, P. A. and Tokunaga, F. (1996) Vision Res. **36**, 933–939
7 Bennett, A. T. D., Cuthill, I. C., Partridge, J. C. and Meier, E. J. (1996) Nature (London) **380**, 433–435
8 Vlitala, J., Korpimaki, E., Palokangas, P. and Kolvula, M. (1995) Nature (London) **373**, 425–427
9 Bowmaker, J. K., Heath, L. A., Wilkie, S. E. and Hunt, D. M. (1997) Vision Res. **37**, 2183–2194
10 Maier, E. J. and Bowmaker, J. K. (1993) J. Comp. Physiol. A **172**, 295–301
11 Bowmaker, J. K. and Martin, G. R. (1985) J. Comp. Physiol. A **156**, 71–77
12 Bowmaker, J. K., Thorpe, A. and Douglas, R. H. (1991) Vision Res. **31**, 349–352
13 Loew, E. R., Govardovskii, V. I., Rohlich, P. and Szel, A. (1996) Visual Neurosci. **13**, 247–256
14 Jacobs, G. H., Neitz, J. and Deegan, II, J. F. (1991) Nature (London) **353**, 655–656
15 Makino, C. L. and Dodds, R. L. (1996) J. Gen. Physiol. **108**, 27–34
16 Higgins, D. G., Bleasby, A. J. and Fuchs, R. (1992) CABIOS **8**, 189–191
17 Saitou, N. and Nei, M. (1987) Mol. Biol. Evol. **4**, 406–425
18 Vissers, P. M. A. M. and DeGrip, W. J. (1996) FEBS Lett. **396**, 26–30
19 Hendriks, T., Klompmakers, A. A., Daemen, F. J. M. and Bonting, S. L. (1976) Biochim. Biophys. Acta **433**, 271–281
20 Groenendijk, G. W. T., DeGrip, W. J. and Daemen, F. J. M. (1980) Biochim. Biophys. Acta **617**, 430–438
21 Heath, L. A., Wilkie, S. E., Bowmaker, J. K. and Hunt, D. M. (1997) Gene, in the press
22 Barthel, L. K. and Raymond, P. A. (1990) J. Histochem. Cytochem. **38**, 1383–1388
23 Jeffery, G. and Williams, A. (1994) Exp. Eye Res. **100**, 47–57
24 Nathans, J. (1992) Biochemistry **31**, 4923–4931
25 Sakmar, T. P., Franke, R. R. and Khorana, H. G. (1989) Proc. Natl. Acad. Sci. U.S.A. **86**, 8309–8313
26 Janssen, J. J. M., Bovee-Geurts, P. H. M., Merkx, M. and DeGrip, W. J. (1995) J. Biol. Chem. **270**, 11222–11229
27 Harosi, F. I. (1994) Vision Res. **34**, 1359–1367
28 Partridge, J. C. and DeGrip, W. J. (1991) Vision Res. **31**, 619–630
29 Knowles, A. and Dartnell, H. J. A. (1977) in Photobiology of Vision, 2B, The Eye, (Davson, H., ed.), pp. 53–174, Academic Press, New York
30 Nathans, J. (1990) Biochemistry **29**, 9746–9752
31 Merbs, S. L. and Nathans, J. (1993) Photochem. Photobiol. **58**, 706–710
32 Baldwin, J. M. (1993) EMBO J. **12**, 1693–1703
33 Harosi, F. I. and Sandorfy, C. (1995) Photochem. Photobiol. **61**, 510–517
34 Sandorfy, C. and Vocelle, D. (1989) in Molecules in Physics, Chemistry and Biology, vol. IV, (Maruani, J., ed.), pp. 195–211, Kluwer Acad. Pub. Dordrecht, The Netherlands
35 Curcio, C. A., Allen, K. A., Sloan, K. R., Lerea, C. L., Hurley, J. B., Klock, I. B. and Milam, A. H. (1991) J. Comp. Neurology **312**, 610–624
36 Stenkamp, D. L., Hisatomi, O., Barthel, L. K., Tokunaga, F. and Raymond, P. A. (1996) Inv. Ophth. Vis. Sci. **37**, 363–375
37 Ohtsuka, T. (1984) Neurosci. Lett. **52**, 241–245
38 Szel, A., Rohlich, P., Caffe, A. R., Juliusson, B., Aguirre, G. A. and van Veen, T. (1992) J. Comp. Neur. **325**, 327–342